Supporting Information

Thermally Expanded Iron Phthalocyanine Nano-Crystal with Compressed Fe–N Bond Confined in Carbon Nitride for Fenton-like Reaction with Superior Activity and Stability

Jiaxin Li [1], Jiahao Cui [1,2,*], Kun Wang [1], Jiaran Yao [1], Di Meng [1], Wenying Yu [1], Qiang Huang [1] and Yubao Zhao [1,*]

[1] Center for Water Research, Institute of Environment and Health, Department of Chemistry and Environmental Science, Inner Mongolia Normal University, Hohhot 010010, China
[2] School of Municipal and Environmental Engineering, Henan University of Urban Construction, Pingdingshan 467036, China
* Correspondence: cuijh@huuc.edu.cn (J.C.); ybzhao@gzhu.edu.cn (Y.Z.)

Table of Content

Table S1. Percentage of the deconvoluted peaks in the XPS C 1s signal. 3
Table S2. Percentage of the deconvoluted peaks in the XPS N 1s signal. 3
Table S3. Percentage of the C, N, and O determined by X-ray photoelectron spectroscopy. 3
Table S4. Weight percentage of Fe in the single-atom Fe catalysts. 3
Table S5. EXAFS fitting parameters for single atom catalysts. 3
Table S6. Basic water quality parameters. 3
Table S7. Summary of the recently reported single−atom catalysis for PMS activation. 3
Figure S1. X-ray photoelectron spectroscopic survey scan on FePc@CN-0 and FePc@CN-2. 4
Figure S2. Best-fit of FT-EXAFS spectra in R-space. 4
Figure S3. Pseudo first-order reaction rate constants (*k*) of the reaction catalyzed by a series of single-atom catalysts. 5
Figure S4. Photograph of the fixed-bed flow reactor in operation (*Φ I.D.* = 1.2 cm). 5
Figure S5.XRD of FePc@CN-2 before and after the reaction. 6
Figure S6. (a) The impact of the mineral ions and humic acid on CIP degradation performance on FePc@CN-2. (b) Pseudo first-order reaction rate constants (*k*) of the reaction. 6
Figure S7. Catalytic performance of FePc@CN-2 in various pH. 6
Figure S8. Catalytic performance of FePc@CN-2 in various water systems. 7
Figure S9. I−t (current-time) curves changes upon sequential addition of PMS and CIP. 7
Figure S10. Reaction equation of MPSO to $MPSO_2$ probe reaction. 7
Reference 7

Table S1. Percentage of the deconvoluted peaks in the XPS C 1s signal.

Entry	Component	Percentage (%)	
		FePc@CN-0	FePc@CN-2
1	C=C	61.6	61.0
2	C−O	25.2	21.1
3	C=N/O	13.2	17.9

Table S2. Percentage of the deconvoluted peaks in the XPS N 1s signal.

Entry	Component	Percentage (%)	
		FePc@CN-0	FePc@CN-2
1	Pyridinic N	57.7	67.3
2	Pyrrolic N	42.3	32.7

Table S3. Percentage of the C, N, and O determined by X-ray photoelectron spectroscopy.

Items	Percentage (%)	
	FePc@CN-0	FePc@CN-2
C	54.1	54.5
N	37.4	29.6
O	10.5	15.7
C/N	1.4	1.8

Table S4. Weight percentage of Fe in the single-atom Fe catalysts.

Catalysts	Fe loadings (wt. %)
FePc@CN-0	4.5
FePc@CN-1	6.1
FePc@CN-2	5.1
FePc@CN-3	3.7

Table S5. EXAFS fitting parameters for single atom catalysts.

Catalysts	Shell	CN [a]	R (Å) [b]	σ^2 (Å^2) [c]	ΔE_0 (eV) [d]	R factor [e]
FePc@CN-0	Fe—N	4.1	2.19	0.0105	-0.742	0.0122
FePc@CN-2	Fe—N	4.0	1.92	0.0099	0.574	0.0102

[a] CN: Coordination number. [b] R: Bond length. [c] σ^2: Debye-Waller factor. [d] ΔE_0: the inner potential correction. [e] R factor: the goodness of fitting.

Table S6. Basic water quality parameters.

Water	pH	Conductivity/μs cm^{-1}	TOC/ppm
Tap Water	8.03	34.1	2.3
ZhuJiang River	7.51	26.1	24.4

Table S7. Summary of the recently reported single−atom catalysis for PMS activation.

Catalyst (g L^{-1})	Pollutant (mg L^{-1})	PMS (mM)	k_{obs} (min^{-1})	k_{value} (min^{-1} L^{-1} mM^{-1})	References
FePc@CN-2 (0.06)	5	0.5	0.49	81.6	This work
Fe-N-O-GC (0.1)	10	0.4	0.24	60	[1]
ZnO@SA-Co-CN (0.1)	20	2.0	0.52	52	[2]
Fe-N-C (0.1)	14.56	0.5	0.17	49.5	[3]
Co-SA (0.2)	20	0.5	0.11	22	[4]
Fe_{SA}-BNC (0.1)	0.45	0.2	1.60	36	[5]
FeN_x-C(0.2)	20	0.5	0.36	72	[6]
Co-TiO_2 (0.1)	20	0.3	0.11	73.3	[7]
CoPc/G-NH2 (0.02)	0.94	0.2	0.29	68.2	[8]
FeBi−N-C (0.1)	10	1.7	0.26	14.7	[9]

Fe-N_4C (0.1)	20	1.0	0.05	10	[10]
Fe-SAC-41.31 (0.1)	10	2.0	1.06	53	[11]

The k_{value} in this work refers to the modification value of k_{obs}, and it can be obtained from the equation : $k_{\text{value}} = \frac{k_{\text{obs}} \times c_{[\text{pollutant}]}}{c_{[\text{catalyst}]} \times c_{[\text{PMS}]}}$.

Where k_{obs} is Pseudo first-order reaction rate constants, min^{-1}; $c_{[\text{pollutant}]}$ is the concentration of pollutant, mg L^{-1}; $c_{[\text{catalyst}]}$ is the concentration of catalyst, g L^{-1}; $c_{[\text{PMS}]}$ is the concentration of PMS, mM.

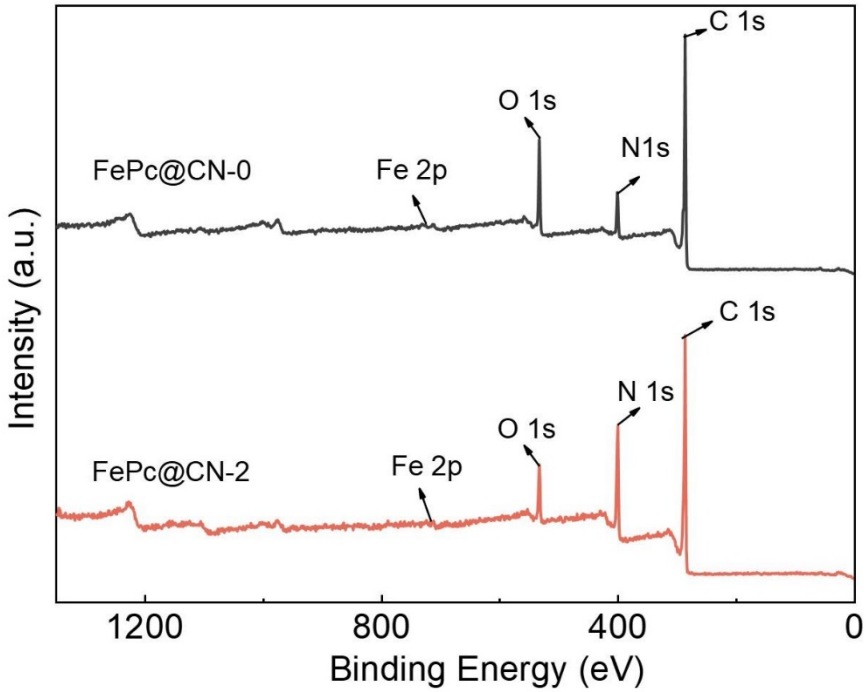


Figure S1. X-ray photoelectron spectroscopic survey scan on FePc@CN-0 and FePc@CN-2.

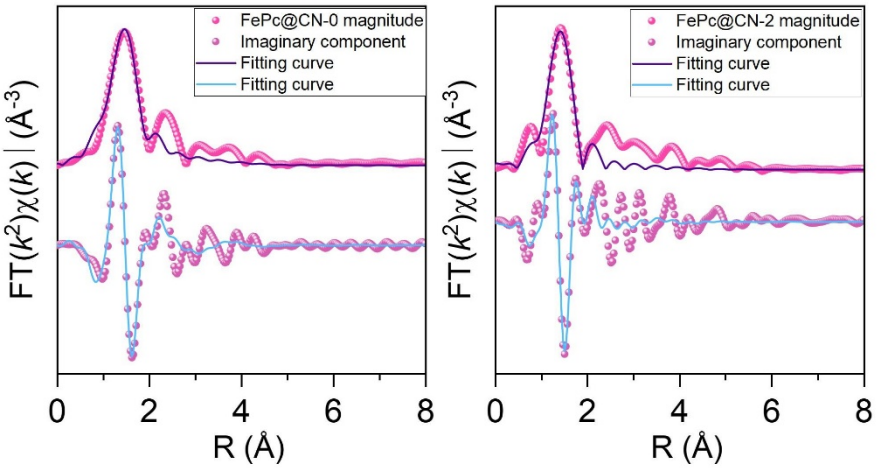


Figure S2. Best-fit of FT-EXAFS spectra in R-space.

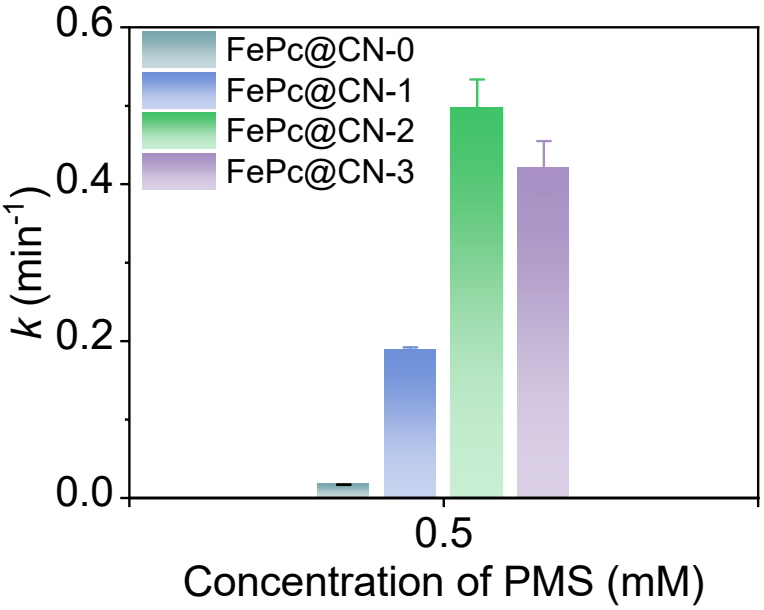


Figure S3. Pseudo first-order reaction rate constants (*k*) of the reaction catalyzed by a series of single-atom catalysts.

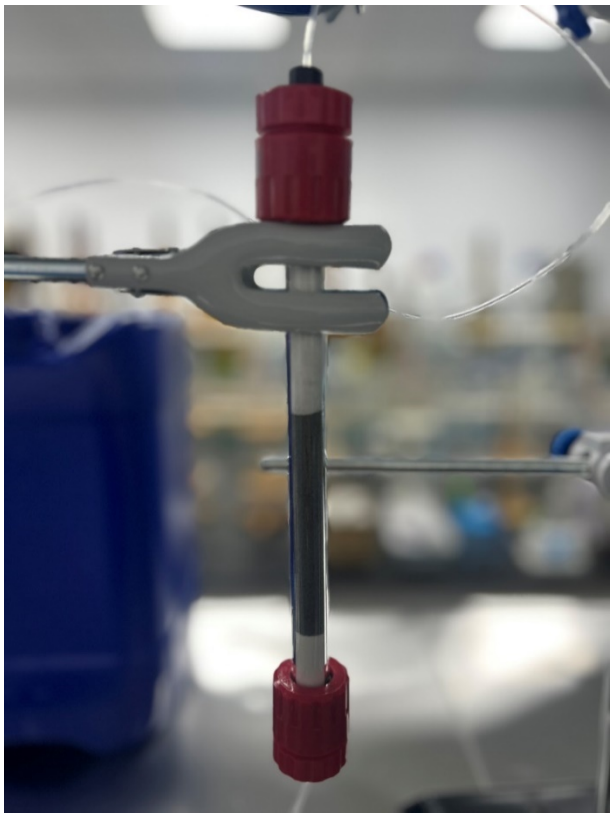


Figure S4. Photograph of the fixed-bed flow reactor in operation (*Φ I.D.* = 1.2 cm).

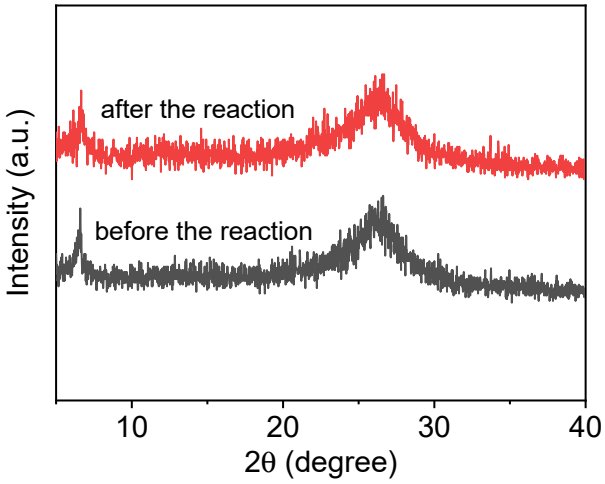


Figure S5. XRD of FePc@CN-2 before and after the reaction.

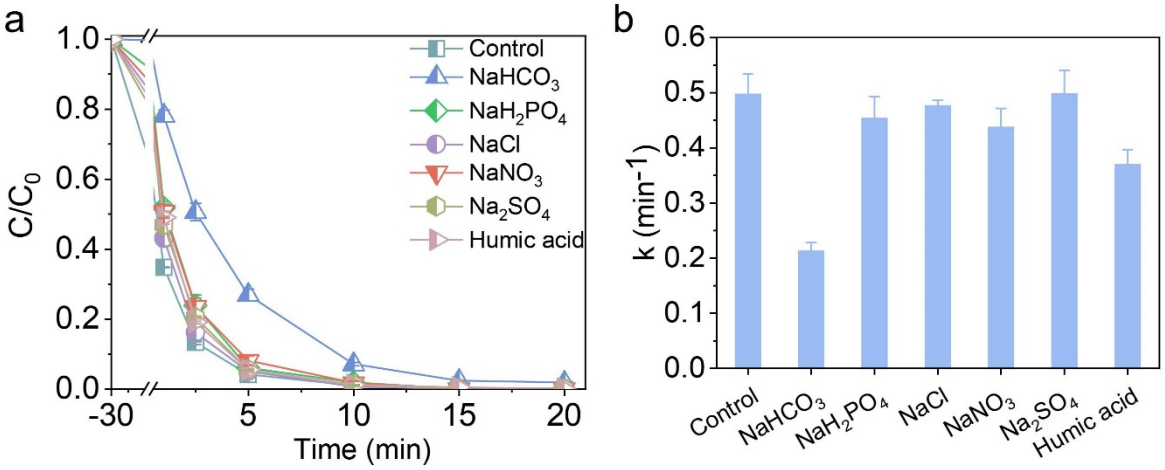


Figure S6. (a) The impact of the mineral ions and humic acid on CIP degradation performance on FePc@CN-2. (b) Pseudo first-order reaction rate constants (k) of the reaction. Reaction conditions: [CIP] = 5 mg L^{-1}, [PMS] = 0.5 mM, [catalyst] = 0.06 g L^{-1}, [Humic acid] = 5 ppm, [mineral ions] = 5 mM.

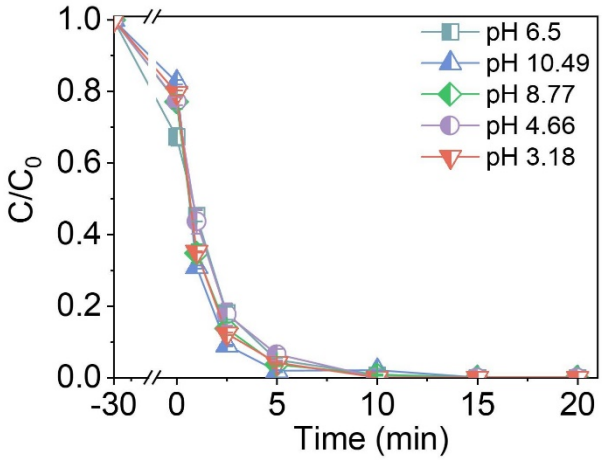


Figure S7. Catalytic performance of FePc@CN-2 in various pH. Reaction conditions: [CIP] = 5 mg L^{-1}, [PMS] = 0.5 mM, [catalyst] = 0.06 g L^{-1}.

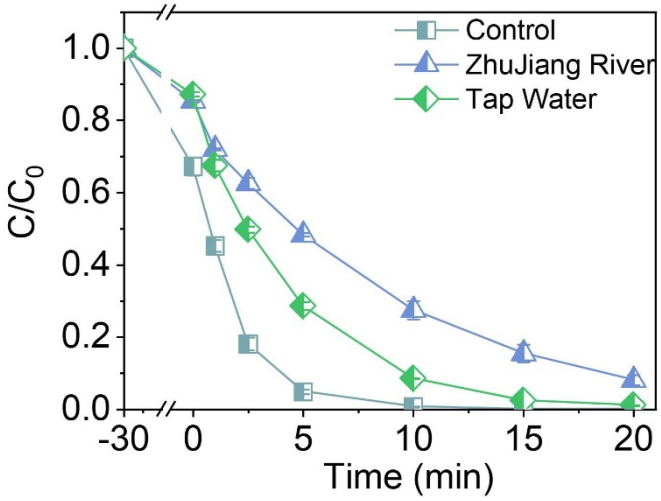


Figure S8. Catalytic performance of FePc@CN-2 in various water systems. Reaction conditions: [CIP] = 5 mg L^{-1}, [PMS] = 0.5 mM, [catalyst] = 0.06 g L^{-1}.

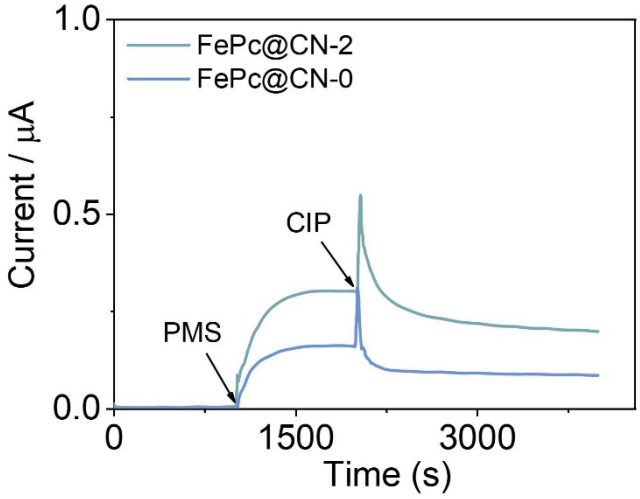
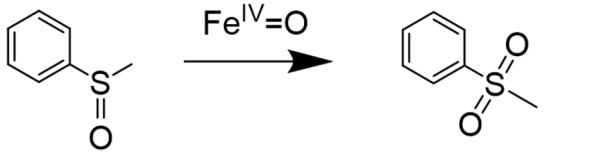


Figure S9. I−t (current-time) curves changes upon sequential addition of PMS and CIP. Working electrode surface area = 1 cm^2, Init E (V) = 0.2, Sample Interval (s) = 0.1, Run Time (s) = 4000, Sensitivity (A/V) = 0.001. Add PMS at 1000 seconds, then add CIP at 2000 seconds.



Methyl phenyl sulfoxide (MPSO) — Methyl phenyl sulfone ($MPSO_2$)

Figure S10. Reaction equation of MPSO to $MPSO_2$ probe reaction.

Reference

1. Wang, S.; Xu, L.; Wang, J. Iron-based dual active site-mediated peroxymonosulfate activation for the degradation of emerging organic pollutants. *Environ. Sci. Technol.* **2021**, *55*, 15412–15422.

2. Wu, X.L.; Liu, S.; Li, Y.; et al. Directional and Ultrafast Charge Transfer in Oxygen-Vacancy-Rich ZnO@Single-Atom Cobalt Core-Shell Junction for Photo-Fenton-Like Reaction. *Angew. Chem. Int. Ed.* **2023**, *62*, 202305639.
3. Cheng, C.; Ren, W.; Miao, F.; et al. Generation of FeIV=O and its Contribution to Fenton-Like Reactions on a Single-Atom Iron−N−C Catalyst. *Angew. Chem. Int. Ed.* **2023**, *62*, 202218510.
4. Mi, X.; Wang, P.; Xu, S.; et al. Almost 100 % Peroxymonosulfate Conversion to Singlet Oxygen on Single-Atom CoN_{2+2} Sites. *Angew. Chem. Int. Ed.* **2021**, *60*, 4588–4593.
5. Deng, Y.; Zhou, Y.; Song, Z.; et al. Long-Range Electronically Polarized Fe-N_5 Catalysts Redirect Polymerization-Driven Phenolic Pollutant Removal Toward Sustainable Carbon Sequestration. *Angew. Chem. Int. Ed.* **2025**, *64*, 202509493.
6. Zhang, B.; Li, X.; Akiyama, K.; et al. Elucidating the mechanistic origin of aspin state-dependent FeN_x–C catalyst toward organic contaminant oxidation via peroxymonosulfate activation. *Environ. Sci. Technol*. **2021**, *56*, 1321–1330.
7. Ye, F.; Wang, J.-R.; Ding, Y.; et al. Photoswitching-Modulated Interfacial Electron Transfer in Single-Atom Co-TiO2 for Enhanced Pollutant Mineralization in Persulfate-Based AOPs. *Environ. Sci. Technol.* **2025**, *59*, 17869–17880
8. Huang, B.; Ren, X.; Zhao, J.; et al. Modulating Electronic Structure Engineering of Atomically Dispersed Cobalt Catalyst in Fenton-like Reaction for Efficient Degradation of Organic Pollutants. *Environ. Sci. Technol.* **2023**, *57*, 14071–14081.
9. Zhao, Z.; Dai, H.; Nie, T.; et al. Dynamic electronic modulation of single-atom Fe sites with p-block metal coordination enables highly selective generation of FeIV = O in Fenton-like reactions. *Nat. Commun.* **2025**, *16*, 11290.
10. Zhu, K.; Wang, L.; Hu, Z.; et al. Curved interface-induced Jahn-Teller effect in single-atom catalysts for water purification. *Nat. Commun.* **2025**, *16*, 11047.
11. Li, S.; Wang, W.; Wu, H.; et al. Facile cascade-anchored synthesis of ultrahigh metal loading single-atom for significantly improved Fenton-like catalysis. *Nat. Commun.* **2025**, *16*, 8796.